REPORT DOCUMENTATION PAGE

Form Approved OMB NO. 0704-0188

1. REPORT DATE (DD-MM-YYYY)	2. REPORT TYPE	3. DATES COVERED (From - To)
20-04-2017	Final Report	1-Oct-2015 - 30-Sep-2016

4. TITLE AND SUBTITLE
Final Report: Investigation of Dynamic Effects and Coherence Limits of Hybrid Si/III-V Lasers

5a. CONTRACT NUMBER
W911NF-15-1-0584

5b. GRANT NUMBER

5c. PROGRAM ELEMENT NUMBER
611102

5d. PROJECT NUMBER

5e. TASK NUMBER

5f. WORK UNIT NUMBER

6. AUTHORS
Amnon Yariv, Mark Harfouche

7. PERFORMING ORGANIZATION NAMES AND ADDRESSES
California Institute of Technology
Office of Sponsored Research
1200 E. California Blvd.
Pasadena, CA 91125 -0001

8. PERFORMING ORGANIZATION REPORT NUMBER

9. SPONSORING/MONITORING AGENCY NAME(S) AND ADDRESS (ES)
U.S. Army Research Office
P.O. Box 12211
Research Triangle Park, NC 27709-2211

10. SPONSOR/MONITOR'S ACRONYM(S)
ARO

11. SPONSOR/MONITOR'S REPORT NUMBER(S)
67994-EL.1

12. DISTRIBUTION AVAILIBILITY STATEMENT
Approved for Public Release; Distribution Unlimited

13. SUPPLEMENTARY NOTES
The views, opinions and/or findings contained in this report are those of the author(s) and should not contrued as an official Department of the Army position, policy or decision, unless so designated by other documentation.

14. ABSTRACT
We have achieved the 3 tasks we set out to complete:
1. We dramatically improved the performance of the frequency noise power spectral density measurement setup allowing measurement to be taken at 300 MHz. This enabled the measurement of a sub kHz Schawlow-Townes linewidth.
2. We have theoretically and experimentally investigated the limits of high coherence Si-III/V lasers considering

15. SUBJECT TERMS

16. SECURITY CLASSIFICATION OF: a. REPORT	b. ABSTRACT	c. THIS PAGE	17. LIMITATION OF ABSTRACT	15. NUMBER OF PAGES	19a. NAME OF RESPONSIBLE PERSON
UU	UU	UU	UU		Amnon Yariv
					19b. TELEPHONE NUMBER 626-395-4821

Standard Form 298 (Rev 8/98)
Prescribed by ANSI Std. Z39.18

Report Title

Final Report: Investigation of Dynamic Effects and Coherence Limits of Hybrid Si/III-V Lasers

ABSTRACT

We have achieved the 3 tasks we set out to complete:

1. We dramatically improved the performance of the frequency noise power spectral density measurement setup allowing measurement to be taken at 300 MHz. This enabled the measurement of a sub kHz Schawlow-Townes linewidth.
2. We have theoretically and experimentally investigated the limits of high coherence Si-III/V lasers considering non-linearities that exist in Si. We have found that while the coherence of these lasers can be increased by moving a larger fraction of the light from the high loss III/V to the low loss Si, FCA and TPA limit the output power and external efficiency of the lasers. We also proposed methodologies to overcome limitations imposed by FCA and TPA while still using silicon as a photon storage device.
3. We have investigated the modulation characteristics of the Si-III/V lasers.

It might be advantageous to consider enabling heterogeneously integrated lasers on different materials platforms to avoid non-linearities present in silicon.

Enter List of papers submitted or published that acknowledge ARO support from the start of the project to the date of this printing. List the papers, including journal references, in the following categories:

(a) Papers published in peer-reviewed journals (N/A for none)

Received Paper

TOTAL:

Number of Papers published in peer-reviewed journals:

(b) Papers published in non-peer-reviewed journals (N/A for none)

Received Paper

TOTAL:

Number of Papers published in non peer-reviewed journals:

(c) Presentations

Number of Presentations:

Non Peer-Reviewed Conference Proceeding publications (other than abstracts):

Received Paper

TOTAL:

Number of Non Peer-Reviewed Conference Proceeding publications (other than abstracts):

Peer-Reviewed Conference Proceeding publications (other than abstracts):

Received Paper

TOTAL:

Number of Peer-Reviewed Conference Proceeding publications (other than abstracts):

(d) Manuscripts

Received Paper

TOTAL:

Number of Manuscripts:

Books

Received Book

TOTAL:

Received Book Chapter

TOTAL:

Patents Submitted

Patents Awarded

Awards

Graduate Students

NAME	PERCENT_SUPPORTED	DISCIPLINE
Mark Harfouche	32	Electrical Engineering
Dongwan Kim	25	Applied Physics
FTE Equivalent:	**0.57**	
Total Number:	**2**	

Names of Post Doctorates

NAME	PERCENT_SUPPORTED
FTE Equivalent:	
Total Number:	

Names of Faculty Supported

NAME	PERCENT_SUPPORTED	National Academy Member
Dr. Amnon Yariv	0.01	Yes
FTE Equivalent:	**0.01**	
Total Number:	**1**	

Names of Under Graduate students supported

NAME	PERCENT_SUPPORTED
FTE Equivalent:	
Total Number:	

Student Metrics

This section only applies to graduating undergraduates supported by this agreement in this reporting period

The number of undergraduates funded by this agreement who graduated during this period: ......

The number of undergraduates funded by this agreement who graduated during this period with a degree in science, mathematics, engineering, or technology fields:......

The number of undergraduates funded by your agreement who graduated during this period and will continue to pursue a graduate or Ph.D. degree in science, mathematics, engineering, or technology fields:......

Number of graduating undergraduates who achieved a 3.5 GPA to 4.0 (4.0 max scale):......

Number of graduating undergraduates funded by a DoD funded Center of Excellence grant for Education, Research and Engineering:......

The number of undergraduates funded by your agreement who graduated during this period and intend to work for the Department of Defense ......

The number of undergraduates funded by your agreement who graduated during this period and will receive scholarships or fellowships for further studies in science, mathematics, engineering or technology fields: ......

Names of Personnel receiving masters degrees

NAME

Total Number:

Names of personnel receiving PHDs

NAME

Total Number:

Names of other research staff

NAME	PERCENT_SUPPORTED
Kevin Cooper	0.38
FTE Equivalent:	**0.38**
Total Number:	**1**

Sub Contractors (DD882)

Inventions (DD882)

Scientific Progress

Technology Transfer

Investigation of Dynamic Effects and Coherence Limits of Hybrid Si/III-V Lasers

(W911NF-15-1-0584)
Final report: 12/30/16

Final report (Oct 2015 – Oct 2016)

Caltech PI: Dr. Amnon Yariv (ayariv@caltech.edu)

Government Team

DARPA:

Grants Officer's Representative

Dr. Michael D. Gerhold (919) 549-4357 (michael.d.gerhold.civ@mail.mil)

High Level Summary

Statement of Work

1. Measure the actual laser noise-floor by overcoming instrumentation noise which previously dominated the noise spectrum.
2. Analyze the theoretical limits of noise performance. Here, we will investigate the role of two-photon-absorption (TPA) and the attendant free-carriers in silicon with regards to laser-noise.
3. Study laser dynamics, both theoretically and experimentally. We will investigate the impact of nonlinear effects and the unique design approach on the intensity and frequency modulation response.

Schedule:	October 01 2015 to October 01 2016
Resources:	All equipment in house.
Scope:	To investigate measure the noise floor of high coherence semiconductor lasers in the presence of non-linearities in silicon.

Conclusions

In conclusion, we have achieved the 3 tasks we set out to complete:

1. We dramatically improved the performance of the frequency noise power spectral density measurement setup allowing measurement to be taken at 300 MHz. This enabled the measurement of a sub kHz Schawlow-Townes linewidth.
2. We have theoretically and experimentally investigated the limits of high coherence Si-III/V lasers considering non-linearities that exist in Si. We have found that while the coherence of these lasers can be increased by moving a larger fraction of the light from the high loss III/V to the low loss Si, FCA and TPA limit the output power and external efficiency of the lasers. We also proposed methodologies to overcome limitations imposed by FCA and TPA while still using silicon as a photon storage device.
3. We have investigated the modulation characteristics of the Si-III/V lasers. These lasers exhibit a unique frequency modulation response due to the presence of FCA and TPA absorption.

While decreasing the effects of non-linearities in silicon is possible, it might be advantageous to work toward enabling heterogeneously integrated lasers on different materials platforms. There is a great need to theoretically and experimentally investigate new semiconductor materials that may be able to circumvent the limitations imposed by the silicon layer to get rid of FCA and TPA for the next generation of high coherence lasers. Such materials pose interesting challenges as few semiconductor materials exists with a refractive index larger than that of InP used to generate photons.

Technical Status:

Task 1: Measure the actual laser noise-floor by overcoming instrumentation noise which previously dominated the noise spectrum.

Previously, the measured frequency noise power spectral density (PSD) was dominated by classical thermal noise due. This was in part due to the fact that the measurement was limited to frequencies below 100 MHz [1]. To extend the measurement to 0.3 GHz, where thermal noise is lower in magnitude, one needs to ensure that relative intensity noise (RIN) is lower than the frequency noise power spectral density. It can be shown that as the measurement of the frequency noise PSD is extended to higher RF frequencies, the frequency noise PSD is proportional to $1/f_{meas}^2$ where f_{meas} is the radio frequency at which the measurement of the frequency noise floor is taken. Therefore, to extend the frequency noise PSD measurement to a higher frequency where classical is not limiting the measurement, RIN needs to be removed.

Previously, the measurement setup used to measure the frequency noise used a Mach-Zhender interferometer as a frequency discriminator in conjunction with a single ended high speed photo-detector and an electrical spectrum analyzer to measure the frequency noise power spectral density of the laser as shown in Figure 1. Unfortunately, such a scheme measures both the intensity noise and the frequency noise of the laser. It for low noise measurements, it is desirable to utilize a scheme that measures only the frequency noise without the intensity noise of the laser.

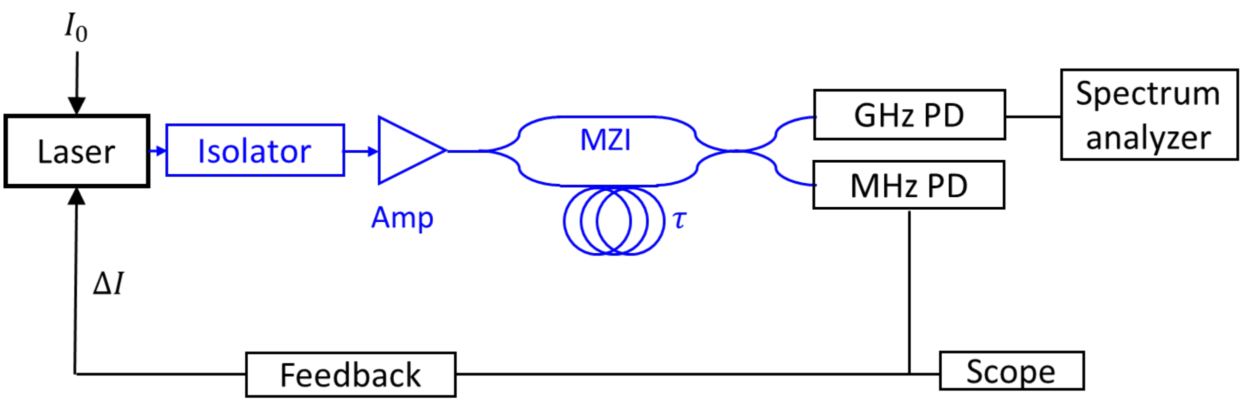

Figure 1. The previous frequency noise measurement setup. All optical couplers in this configuration are 3 dB couplers. In this configuration, the feedback is applied to the laser and the measurement at the GHz photodetector is not balanced. Therefore a large DC term exists due to the relative intensity noise in the laser (RIN). For small path lengths, necessary to measure the frequency noise power spectral density at high frequencies, it is often difficult to differentiate the RIN from the frequency noise PSD. In this setup, the feedback system, described in [PNSA] is used to keep the laser frequency locked to the quadrature point MZI. Without feedback, the quadrature point of the MZI would drift away from the laser output frequency reducing the SNR in the measurement system.

We moved to utilizing a balanced measurement scheme, shown in Figure 2. whereby the signal from both arm of the interferometer is measured on two photodetectors and the respective signals are subtracted. This is known as a balanced interferometer setup. Each arm measures the laser power, and thus the intensity noise, but measures the frequency noise component of the measurement in each arm has a different sign. Thus, after subtracting both measured signals on the interferometer, only the frequency noise remains. This allows us to measure the frequency noise power spectral density up to approximately 0.3 GHz at which point the measurement becomes limited by the dark noise of the detector. This allows us to extract the well-known Schawlow-Townes linewidth, in other words the quantum limited frequency noise power spectral density.

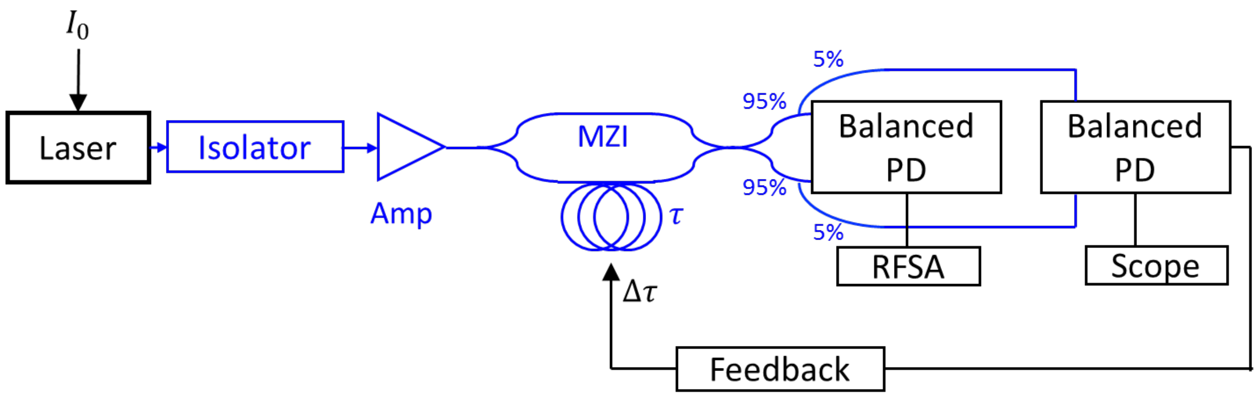

Figure 2. Frequency noise power spectral density measurement utilizing a balanced photodetector. The use of a balanced photodetector (output of the device is equal to the difference of the electrical signal of both arms of the MZI) means that the RIN is heavily suppressed in the measurement. In this case, feedback acts on the path length of the MZI (changing it by a less than a few microns compared to a path length mismatch of 10s of mm) to ensure that the optical frequency of the laser stays at the quadrature point of the MZI for the duration of the measurement.

Using this scheme, we measured the frequency noise power spectral of lasers with 3 different thickness of quantum noise control layers. Figure 3 depicts the important physical characteristics of the cross section of the lasers while Figure 4 shows the general structure of the lasers. The quantum noise control layer, composed of SiO_2 enables a large reduction in the frequency noise power spectral by decreasing spontaneous emission. With this scheme, the output power is left unchanged as lasers with increased thickness of SiO_2 have a larger quality factor and thus are able to store more photons resulting in a constant stimulated emission rate for different thicknesses of SiO2 [2,3]. The measurements of the frequency noise power spectral density are summarized in Figure 4. Using quantum noise control layers of 30 nm, 100 nm, and 150 nm, quantum limited linewidths of 30 kHz, 2.5 kHz, and 1.4 kHz are respectively obtained by estimating the white noise level of the traces in Figure 4. The measurement the differentiation of the linewidth between the 100 nm and 150 nm thicknesses of quantum control layers is enabled by the fact that we can now measure the frequency noise power spectral density.

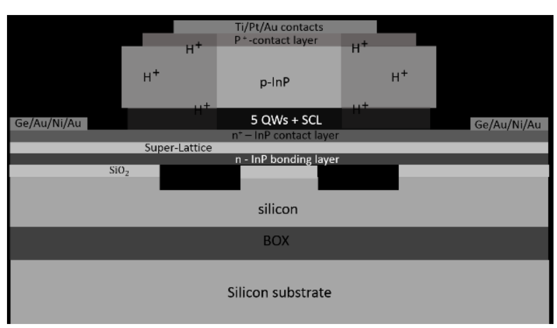

Figure 3. General structure of the high coherence heterogenously integrated Si/III-V lasers. The SiO2 layer between the Si and the n-doped InP is known as the quantum noise control layer. The thickness of this layer determines the fraction of optical power in the low loss silicon compared to the fraction of optical power interacting with the high-loss InP.

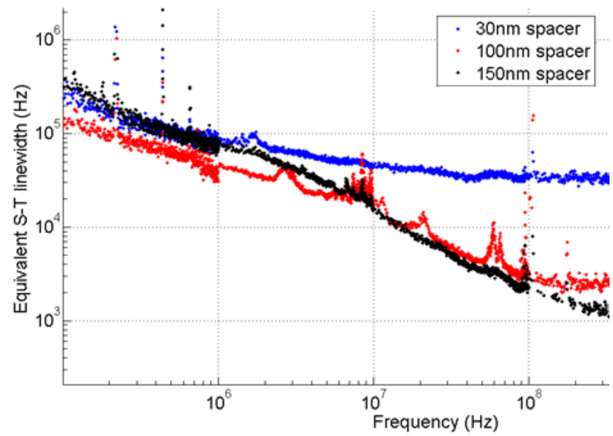

Figure 4. Measurement of the frequency noise PSD of lasers with different thicknesses of quantum noise control layers. The measurement of the white noise floor is estimated at 300 MHz. Above 300 MHz, the dark noise of the balanced photodetector dominated the measurement. In this particular case, measurements are taken at a bias current 33 mA above threshold for all lasers.

Task 2. Limits of quantum noise control in heterogeneously integrated Si-III/V lasers considering non-linearities

Two photon absorption (TPA) and free carrier absorption (FCA) can impact laser performance and dynamics. To investigate these effects, we modify the well-known rate equations to include an equation for free carriers in silicon as well as two photon and free carrier absorption of photons. The following equation describes the free carrier density (n_{Si}) in the silicon as well as the densities of the electron-hole pairs in the quantum wells (n_e) and the photon density (n_p) [4]:

$$\frac{dn_e}{dt} = \frac{n_e}{\tau_r} - \frac{\Gamma_{\mathrm{QW}}}{\Gamma_{\mathrm{Geom}}} G_m(n_e)n_p + \frac{\eta I}{qV_{QW}}$$

$$\frac{dn_p}{dt} = \left(\Gamma_{QW}G_m(n_e) - \alpha\right)n_p - \beta_T h\nu v_g M_{TPA}\Gamma_{Si}^2 n_p^2 - v_g\sigma_a n_{Si}\Gamma_{Si}n_p$$

$$\frac{dn_{Si}}{dt} = \frac{1}{2}\beta_T h\nu v_g^2 M_{TPA}\Gamma_{Si}n_p^2 - \frac{n_{Si}}{\tau_{eff}}$$

most parameters used in the equation are summarized in Table 1 [cite yasha]. β_T is defined as the coefficient that relates the change of the imaginary part of the refractive index $\Delta n_i = \frac{c}{2\omega}\beta_T I$, where c is the speed of light in free space, and ω the angular frequency of emission and I the intensity of light in $\mathrm{W/m^2}$. τ_{eff} is the effective lifetime that the electrons in the silicon interact with the optical mode taking into account lateral diffusion in the silicon as well as surface recombination and bulk recombination lifetimes. M_{TPA} is a constant that relates how uniform the mode is in silicon and allows us to describe non-linear processes without keeping track of the modal field distribution in the waveguide throughout the calculations. M_{TPA} is defined as:

$$M_{TPA} = V_p \frac{\int_{Si} |E(r)|^4 d^3r}{\left(\int_{\mathrm{Si}} |E(r)|^2 d^3r\right)^2},$$

$E(r)$ is the electric field and both integrals are over the full volume of the silicon only. This helps ensure that we take into account the Gaussian-like distribution of the field along the waveguide [2].

Parameter	Description	Value
$\boldsymbol{n_e}$	Electron-hole pair density in the quantum wells	$\cdot\ \mathrm{m}^{-3}$
$\boldsymbol{n_p}$	Photon density	$\cdot\ \mathrm{m}^{-3}$
$\boldsymbol{n_{Si}}$	Free carrier density in the silicon	$\cdot\ \mathrm{m}^{-3}$
$\boldsymbol{\tau_r}$	Electron-hole recombination lifetime (including non-radiative recombination)	$1\ \mathrm{ns}$
$\boldsymbol{G_m}$	Material gain	$2v_g G'_m(n_e - n_{tr})$
$\boldsymbol{G'_m}$	Material differential gain	$1 \times 10^{-19}\ \mathrm{m}^2$
$\boldsymbol{n_{tr}}$	Transparency carrier density	$2 \times 10^{24}\ m^3$
$\boldsymbol{\eta}$	Internal quantum efficiency (including current leakage)	0.3
$\boldsymbol{I}$	Pump current	0 to $200\ \mathrm{mA}$
$\boldsymbol{V_{QW}}$	Quantum well effective volume	$4.2 \times 10^{-17}\ \mathrm{m}^3$
$\boldsymbol{\alpha}$	Linear loss rate in the waveguide	$2\pi\nu/Q$
$\boldsymbol{Q}$	Modal quality factor (linear loss only) -- increases with oxide thickness	1×10^4 to 1×10^6
$\boldsymbol{\beta_T}$	TPA coefficient	$5 \times 10^{-12}\ \mathrm{m/W}$
$\boldsymbol{v_g}$	Mode's group velocity	c/n_g
$\boldsymbol{n_g}$	Group index	3.3
$\boldsymbol{\sigma_a}$	FCA cross section	$1.45 \times 10^{-21}\ \mathrm{m}^2$
$\boldsymbol{\tau_{eff}}$	effective lifetime that the electrons in the silicon interact with the optical mode taking into account lateral diffusion in the silicon as well as surface recombination and bulk recombination lifetimes	$30\ \mathrm{ns}$
$\boldsymbol{M_{TPA}}$	TPA magnification factor	3
$\boldsymbol{\Gamma_{Si}}$	Silicon confinement factor	$\approx .80$
$\boldsymbol{\Gamma_{\mathrm{QW}}}$	Quantum well confinement factor, decreases with oxide thickness	$0.01 - 0.0007$
$\boldsymbol{\Gamma_{\mathrm{Geom}}}$	Ratio between the volume of the quantum wells and the modal volume	$\boldsymbol{\Gamma_{\mathrm{QW}}}/\Gamma_{\mathrm{Si}}$
$\boldsymbol{h}$	Planck's constant	$6.62 \times 10^{-34}\ \mathrm{J \cdot s}$
$\boldsymbol{\nu}$	Optical frequency	$193\ \mathrm{THz}$
$\boldsymbol{c}$	Speed of light	$3 \times 10^8\ \mathrm{m/s}$

Using the equations above, we can solve the steady state output power of the laser in the presence of non-linearity and make theoretical predictions. For a large quantum noise control layer, yielding a laser with the highest cold cavity quality factor, and thus the narrowest linewidth, we find that that the dominant source of loss becomes FCA as illustrated in Figure 5. Even for moderate pump electrical currents, the output power decreases dramatically from the expected value obtained ignoring non-linear effects.

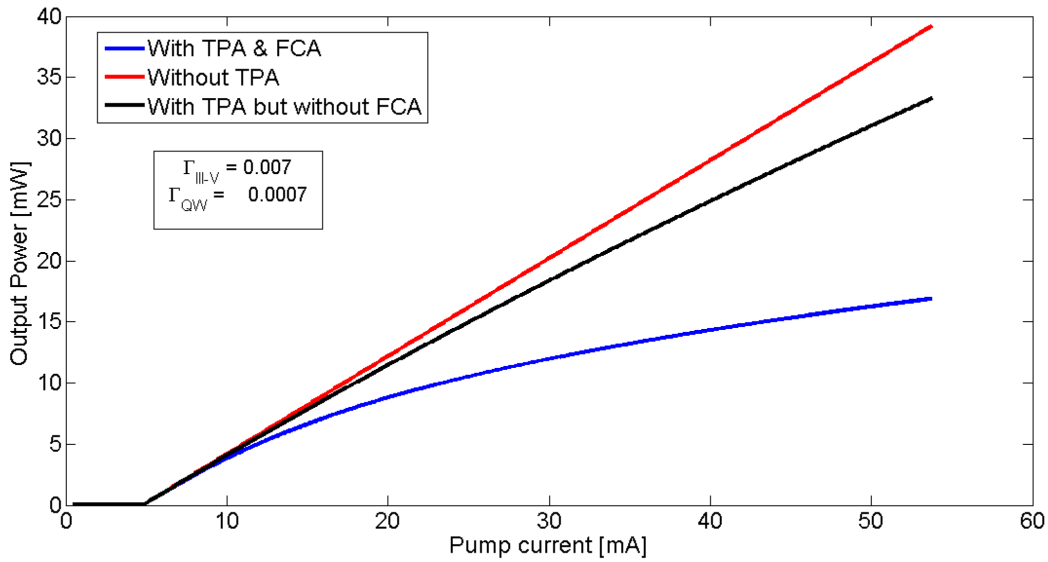

Figure 5. Theoretically predicted luminosity vs intensity characteristics of a heterogeneously integrated Si-III/V laser for a laser with a large (150 nm in this case) quantum noise control layer. If the presence of two photon absorption and free carrier absorption are taken into account, the output power is shown to rapidly saturate.

We experimentally verify these predictions by measuring the DC output characteristics of lasers constructed with different thicknesses of quantum control layers. As expected, for a large oxide thickness between the silicon and the III-V material, the output power saturates quickly. Note that this saturation behavior is also observed in pulsed operation where thermal effects can be ignored. To overcome the limitations imposed by FCA in the silicon, we propose a few minor changes the structure of the laser for future iterations:

1. An increased modal volume achieved by increasing the width of the silicon waveguide while decreasing the etch depth in the silicon.
2. Adding imperfections in the silicon by etching far away from optical mode to create recombination centers for the free carriers. This will decrease the FCA lifetime in the silicon without affecting the losses in the optical mode.
3. Incorporating a p-n junction to sweep the FCA away from the optical waveguide thereby decreasing their interaction with the optical mode.

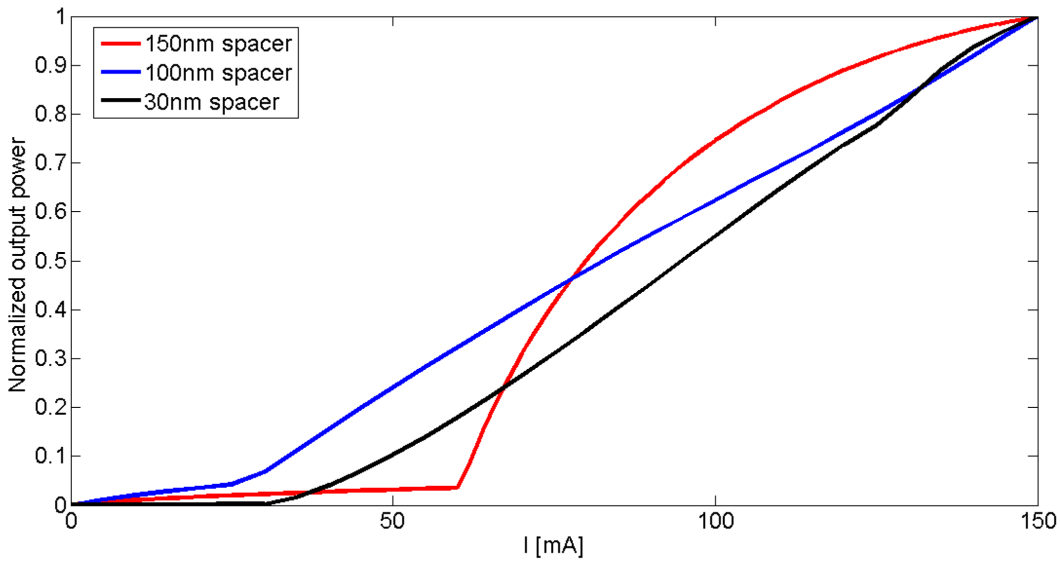

Figure 6. Measured luminosity vs intensity for lasers with different quantum noise control layers (spacer). It is observed that for large thicknesses of quantum noise control layers, the output power rapidly saturates. This is in good agreement with our model for TPA and FCA.

Task 3. Study of laser dynamics in the presence of non-linearities

Presence of the free carrier dynamics also appear in the modulation characteristics of the lasers. While it affects both the intensity modulation response and the frequency modulation response, the frequency modulation response is much more dramatically affected by the presence of FCA than that of the intensity modulation response. As such here we will summarize the results of the frequency modulation response of the laser. It can be found that the change in the optical frequency of the laser relates to the small signal current through:

$$\frac{\Delta\nu}{\Delta I}(s) = \frac{\frac{\alpha_H}{8\pi}\Gamma_{QW}G'_m\frac{\eta_i}{eV_{QW}}\left(s+\frac{1}{\tau_{eff}}\right)\left[s+Bn_{p,0}+\frac{\alpha_T\Gamma_{QW}\epsilon_c n_{p,0}}{1+\Gamma_{QW}\epsilon_c n_{p,0}}\right]+2Cn_{Si,0}}{(s+2\xi\omega_n)\left[\left(s+Bn_{p,0}\right)\left(s+\frac{1}{\tau_{eff}}\right)+2Cn_{Si,0}\right]+\left(s+\frac{1}{\tau_{eff}}\right)\omega_n}$$

Where $s = i\cdot 2\pi\nu_{mod}$, and ν_{mod} and the modulation frequency in Hz and $n_{p,0}$ and $n_{Si,0}$ are the densities of photons and free carriers in the silicon at steady state. Many of the variables were summarized in Table 1. We bring the attention to the presence of the linewidth enhancement factor, α_H which relates fluctuations in the real and imaginary refractive index of the quantum well. e is the charge of an electron. The coefficients B and C relate the non-linear terms in the loss of the cavity to the photon density and the free carrier density through $\alpha_{\text{tot}} = \alpha_{\text{linear}} + Bn_{p,0} + Cn_{Si,0}$.

We summarize the salient features of the theoretically obtained frequency modulation response of the laser shown in Figure 7.

1. For thin 30 nm quantum noise control layer, the response resembles that of a conventional semiconductor laser. This is expected as for such a thin quantum noise control layer the quality factor of the resonator is low enough that non-linearities can be ignored.

2. As the spacer thickness increases, the entire curve maintains in general shape, but decreases in magnitude. This is due to the decreased overlap between the mode and the quantum wells. Changes in the quantum well's refractive index have a smaller effect on the mode due to the low confinement factor.
3. The resonance frequency decreases with increased the quantum noise control layer thickness.
4. For very thick quantum noise control layers, a shallow dip due to the interaction with FCA is revealed at $\omega_{mod} = 1/\tau_{\text{eff}}$. This is due to the fact that the decreased interaction with the III-V increases the Q of the cavity enhancing non-linearities.

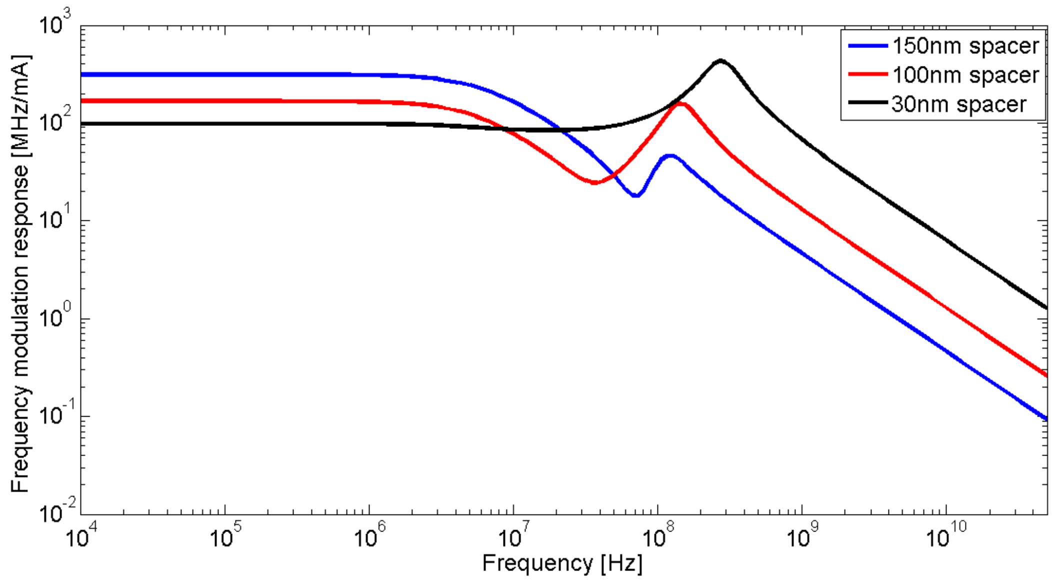

Figure 7. Predicted frequency modulation response for heterogeneously integrated Si-III/V lasers with different thicknesses of quantum noise control layers. The presence of a pole-zero pair is due to the included of TPA and FCA in the rate equations and causes a dip in the frequency modulation response near $10^7 - 10^8$*Hz. This dip become heavily accentuated for large thicknesses of quantum noise control layers.*

We experimentally verified these predictions and show the obtained traces of the modulation response in Figure 8. The same trends, observed in the theoretical predictions of Figure 7 are easily seen. It is important to note that while one might think that the additional pole and zero from the non-linearities might cause problems in directly modulating these lasers, but the presence of this zero-pole pair does not affect external modulators from being used.

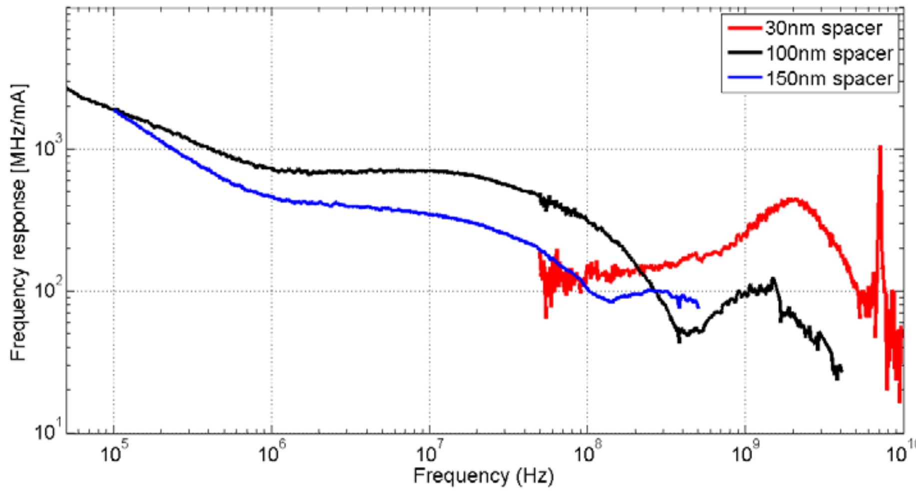

Figure 8. Measured frequency modulation response of heterogeneously integrated Si-III/V lasers with different thicknesses of quantum noise control layers. The larger response in the range of $10^6 - 10^7$ Hz as well as the presence of a dip near 10^8 is consistent with the small signal model of a semiconductor laser including TPA and FCA in the laser rate equations. The identical response near 10^5 Hz is attributed to the thermal frequency modulation response of the laser..

References cited

1. Santis, Christos Theodoros and Steger, Scott T. and Vilenchik, Yaakov et al. (2014) "High-coherence semiconductor lasers based on integral high-Q resonators in hybrid Si/III-V platforms." Proceedings of the National Academy of Sciences of the United States of America, 111 (8). pp. 2879-2884. ISSN 0027-8424
2. Santis, Christos T. and Yariv, Amnon (2015) "High-Q Silicon Resonators For High-Coherence Hybrid Si/III-V Semiconductor Lasers." In: Proceedings CLEO: 2015. Optical Society of America , Art. No. SW3F.6
3. Santis, Christos T. and Vilenchik, Yaakov and Yariv, Amnon et al. (2015) "Sub-kHz Quantum Linewidth Semiconductor Laser On Silicon Chip." In: Proceedings CLEO: 2015. Optical Society of America , Art. No. JTh5A.7.
4. Vilenchik, Yaakov and Santis, Christos T. and Steger, Scott T. et al. (2015) "Theory and observation on non-linear effects limiting the coherence properties of high-Q hybrid Si/III-V lasers." In: Novel In-Plane Semiconductor Lasers XIV. Proceedings of SPIE. No.9382. Society of Photo-Optical Instrumentation Engineers (SPIE) , Bellingham, WA, Art. No. 93820N. ISBN 978-1-62841-472-1